

SURFACE DEFECTS AND CHEMISTRY ON THE $\text{SnO}_2(110)$ SURFACE

David F. Cox
Department of Chemical Engineering
Virginia Polytechnic Institute & State University
Blacksburg, Virginia

SUMMARY

A variety of ultrahigh vacuum (UHV) surface science techniques have been used to characterize the structural, electronic and chemical properties of $\text{SnO}_2(110)$, a model catalytic surface. Two types of surface oxygen vacancies have been identified, each associated with different band gap (defect) electronic states. Adsorption experiments show that the interaction of simple gases with this surface occurs primarily through these oxygen vacancies and can show site-specificity to only one of the two types of vacancies.

INTRODUCTION

Tin oxide (SnO_2) is a useful catalytic material most often applied in multicomponent systems. In mixed-oxide systems, tin oxide has found application in catalysts for selective oxidation, ammoxidation, dehydrogenation and isomerization reactions [1-5]. Pure tin oxide typically forms combustion products [6-9], hence it has found an application as a support for Pt in the low-temperature CO oxidation catalyst for pulsed CO_2 lasers.

One of the primary difficulties in characterizing tin oxide surfaces (and hence Pt/ SnO_2 catalysts) lies in determining the valence state of the surface tin species. It has been found that neither Auger electron spectroscopy (AES) [10-12] or x-ray photoelectron spectroscopy (XPS) [13] can distinguish between Sn^{+2} and Sn^{+4} because there is no significant change in the core-level binding energies. This distinction is important because it characterizes the redox condition of the tin oxide surface which in turn controls its interaction with gas-phase oxygen. In spite of these difficulties, progress has been made in distinguishing between Sn^{+2} and Sn^{+4} using electron loss spectroscopy (ELS) [13,14]. The ELS technique can clearly give a qualitative indication of the presence of Sn^{+2} species in an SnO_2 matrix. ELS is also sensitive to structural changes in the lattice, however, no clear interpretation other than an oxygen deficiency can be associated with the observed spectral changes [14]. In other words, it is impossible to distinguish between a true SnO surface layer and a partially reduced Sn^{+2} containing SnO_2 structures with oxygen vacancies.

These structural ambiguities in surface characterization can be removed by studying model SnO_2 single crystal surfaces. Surface characterization studies of $\text{SnO}_2(110)$ are reviewed here as an example

of the types of information obtainable by studies of well-characterized, model, single-crystal surfaces which cannot be obtained from powders or polycrystalline materials. The (110) face was chosen for these studies because it is the most stable, predominant natural growth face for SnO_2 . Extended high temperature treatments of tin oxide powders and films leads to a preferential growth of (110) faces [15], hence this particular crystal face is the most likely to be a successful model for realistic $\text{SnO}_2(110)$ systems. Also, a perfect (110) crystallographic orientation gives the most "fully oxidized" or "stoichiometric" surface possible because it breaks the fewest number of cation-anion bonds at the surface [16].

BACKGROUND STRUCTURAL INFORMATION

SnO_2 is a wide-band-gap ($E_g=3.6$ eV), n-type semiconductor with the rutile (TiO_2) structure. When viewed along the (110) direction, the bulk crystal is seen to be composed of charge-neutral units containing three atomic planes [17]. The composition and arrangement of the planes in the unit are $[(\text{O}^{2-})(2\text{Sn}^{+4} + 2\text{O}^{2-})(\text{O}^{2-})]$ per (110) unit cell. The charge on each plane is $[(-2)(+4)(-2)]$, and the net charge per three-plane unit is zero. Because this unit has no net dipole moment in the (110) direction, the (110) surface is termed nonpolar. The lower surface energy of a nonpolar vs. a polar surface dictates that an ideal, stoichiometric (110) surface will be terminated by a charge-neutral unit. Terminating the (110) surface with a complete, nonpolar, charge-neutral unit corresponds to breaking the smallest number of cation-anion bonds relative to the bulk structure [16]. This termination results in equal numbers of five and six coordinate tin cations in the second atomic layer. The full bulk coordination per cation is six.

Figure 1 illustrates the structure, composition and charges of the individual atomic planes associated with the $\text{SnO}_2(110)$ surface. From Fig. 1 it can be seen that the ideal (110) surface is terminated with an outermost plane of oxygen anions which appear as rows in the (001) direction and occupy bridging positions between the second-layer, six coordinate tin cations. Oxygen atoms may also be seen in Fig. 1 in the same plane as the observable tin atoms. For convenience, the two different types of oxygen anions are referred to as "bridging" oxygens and "in-plane" oxygens, respectively.

NEARLY STOICHIOMETRIC SURFACES

The preparation of clean, stoichiometric SnO_2 surfaces for study in UHV is nontrivial. The usual cleaning methods of ion bombardment and high temperature annealing in vacuum preferentially remove surface lattice oxygen, leaving the surface in a reduced condition. Attempts to quantify the surface composition following such treatments typically yields O/Sn ratios less than 2.0, indicative of a less than stoichiometric surface [14]. A clear indication of the electronic consequences of the deviation from stoichiometry is the appearance of defect electronic states in the band gap as seen with ultraviolet photoelectron spectroscopy (UPS).

Surface characterization studies [18] have shown that a nearly ideal $\text{SnO}_2(110)$ surface such as that illustrated in Fig. 1 may be reproducibly prepared by sputter cleaning, high temperature annealing in vacuum, and high temperature and pressure oxidation (700 K, 1.0 Torr O_2). The lack of band-gap emission in UPS following such a treatment is a sensitive indicator of a nearly-perfect, stoichiometric (110) surface. Figure 2 illustrates the variations observed in UPS for several surface preparations, including the in-situ oxidation treatment.

Heating the well-oxidized, nearly ideal, stoichiometric (110) surface in UHV removes large amounts of surface lattice oxygen. It has been shown with ion-scattering spectroscopy (ISS) [18] that vacuum annealing a nearly ideal $\text{SnO}_2(110)$ surface at 700 K causes a complete removal of the layer of bridging oxygen anions which terminate the surface, leaving a surface terminated by a tin and oxygen containing plane. In addition to the removal of bridging oxygens and the formation of four coordinate Sn^{+2} cations at 700 K, heating in vacuum above 700 K causes the further removal of some in-plane oxygen from the tin and oxygen containing plane of the $\text{SnO}_2(110)$ surface [18]. The formation of this second type of oxygen vacancy further lowers the coordination number of the neighboring tin cations from five and four coordination to four and three, respectively. Figure 3 is a ball-model illustration showing a nearly-perfect oxidized surface and a surface formed by removal of the top layer bridging oxygens and several in-plane oxygen anions. The figure illustrates the degree to which the composition changes in these treatments, and shows the variety of different coordination numbers of the tin cations.

The sequential fashion in which surface lattice oxygen can be removed from the oxidized $\text{SnO}_2(110)$ surface (bridging oxygen below 800 K, in-plane oxygen above 800 K) makes it possible to tailor this surface in a controlled fashion. The tin cation coordination can be varied from six to three by the proper choice of sample preparation conditions. Associated with these changes in cation coordination, only one surface periodicity is observed in low energy electron diffraction (LEED) when an oxidized surface is used as the starting condition: a (1x1) pattern characteristic of a simple termination of the bulk periodicity. The constancy of the LEED pattern indicates that there is no gross restructuring or reconstruction of the surface associated with the creation of the oxygen vacancies. While there is likely to be some degree of relaxation about the vacancies, the local geometry and coordination is similar to that expected from a simple removal of oxygen atoms from the surface. In essence, the vacancies are created without significantly altering the crystal structure at the surface except by substantial changes in coordination number of the tin cations.

While no changes are observed in the surface geometric structure for these treatments, the surface electronic structure in the band gap undergoes several interesting changes. Associated with the removal of the terminating layer of bridging oxygen anions and the requisite change in coordination of half the surface tin cations from sixfold to fourfold coordination, the appearance of defect electronic states low in the band gap is also observed with UPS. The appearance of these states low in the band gap has been interpreted as the

formation of Sn^{+2} centers associated with the fourfold-coordinated cations [17,18]. For temperatures above 800 K, the formation of threefold-coordinate cations at in-plane oxygen vacancies results in the appearance of a second set of defect electronic states in UPS high in the band gap extending up to the Fermi level. These changes in band-gap electronic structure are illustrated in Figure 4.

HIGHLY OXYGEN-DEFICIENT SURFACES

When ion is bombarded and annealed in vacuum, the SnO_2 (110) surface undergoes a number of reconstructions as characterized by low-energy electron diffraction (LEED) [19,20]. These reconstructions are driven by the high degree of oxygen deficiency associated with the ion-bombarded surface because of the preferential sputtering of oxygen. The most interesting of these reconstructions is the (4x1) surface which is formed by annealing the ion-bombarded surface near 900 K. This particular reconstruction corresponds to the formation of a reduced $\text{SnO}(101)$ coincident overlayer [20] and the reduction of all surface cations to Sn^{+2} oxidation state. Therefore, by the choice of proper surface preparation conditions, a model SnO suboxide surface may also be reproducibly prepared from the SnO_2 (110) surface. For annealing temperatures near 1000 K, the surface exhibits a (1x1) LEED pattern which has the same periodicity as the bulk, and hence approaches the same final condition regardless of whether the starting surface condition was ion bombarded or oxidized.

UPS photoemission studies of the various reconstructions of highly oxygen-deficient SnO_2 (110) surfaces show similar band gap features to those observed for the well-defined (1x1) surface [20]. It has been shown that the conclusions regarding the origin of the band gap features on the well-defined (1x1) surfaces can be generalized for more structurally complex situations. Defect electronic states low in the band gap are associated with fourfold-coordinated Sn^{+2} cations. States higher in the gap are characteristic of oxygen vacancies with neighboring threefold-coordinated Sn cations [20].

SITE-SPECIFIC ADSORPTION OF SIMPLE MOLECULES

The interaction of adsorbates with the electronic states in the band gap provides information about the local geometric and electronic properties of the adsorption sites. The effects of O_2 , H_2 , and H_2O adsorption on the band gap density of states of an ion-sputtered surface are shown with UPS difference curves in Figure 5 [21]. An ion-sputtered surface was chosen for this illustration because it exhibits a large density of states in the band gap when clean. Oxygen adsorption causes a decrease in the photoemission intensity throughout the band gap. Hydrogen adsorption causes a decrease in the defect intensity primarily in states just above the valence band maximum (VBM). A positive change in intensity near the conduction band minimum (CBM) is also seen for hydrogen. This increase is associated with the movement of the Fermi level up in the gap (i.e., downward band bending) and comes from occupied states near the Fermi level for the hydrogen dosed surface. The difference curve

for water shows an increase in the density of states near the Fermi level (as with hydrogen), but a decrease in other states in the top half of the gap. Similar trends are observed for oxygen deficient (4x1) and (1x1) surfaces. The changes in the band-gap density of states caused by H_2 , O_2 , and H_2O indicate that defects associated with oxygen vacancies play an important role in chemisorption on the (110) surface. Additionally, the gases exhibit some specificity between the different electronic states associated with the defect sites.

The previously described assignments for the types of surface defects associated with the band gap electronic states demonstrate that hydrogen and water are site-specific in their interaction with tin oxide surfaces. The interaction of hydrogen with states low in the gap demonstrates that adsorption occurs at fourfold-coordinated cations similar to those found in the presence of bridging oxygen vacancies. The interaction of water with the states high in the band gap demonstrates the adsorption of water at threefold-coordinated cations similar to those associated with in-plane oxygen vacancies.

SITE-SPECIFIC ^{18}O ISOTOPIC LABELING OF THE LATTICE

As with the use of labeled compounds in thermal desorption spectroscopy (TDS), the use of ^{18}O -labeled lattice oxygen at the $SnO_2(110)$ surface provides a means of investigating the interaction of lattice oxygen in surface reactions. The study of isotopic exchange of oxygen with metal oxide catalysts has been widely used, but isotopic exchange with the well-characterized $SnO_2(110)$ surface provides the unusual possibility of labeling not just surface lattice oxygen in general, but the labeling of only one of two different forms of lattice oxygen at the (110) surface with ^{18}O .

Unlike TiO_2 , the diffusion of lattice oxygen through the SnO_2 matrix is slow at temperatures as high as 1000 K, as evidenced by the inability to form a stoichiometric or near-stoichiometric $SnO_2(110)$ surface by simply heating in vacuum after ion bombardment [20]. Therefore, at the 700 K temperatures required for the in situ oxidation treatment [18,20], interlayer mixing of oxygen atoms is expected to be small. Recent ISS results [22] have shown that it is possible to selectively label bridging oxygen positions with ^{18}O , since the two forms of surface lattice oxygen can be removed sequentially by heating to different temperatures in UHV. The labeling procedure will make it possible to distinguish between the participation of the two inequivalent forms of lattice oxygen in surface oxidation reactions using TDS.

COMPARISON BETWEEN EXISTING CATALYTIC DATA AND THE SURFACE PROPERTIES OF $SnO_2(110)$

The previous work on CO oxidation and NO reduction [6-9,23,24] offers insight into the role of SnO_2 in catalyzing oxidation/reduction reactions. The studies using pure tin oxide show that a redox mechanism dominates the chemistry at the surface of SnO_2 . CO is converted to CO_2 on oxidized SnO_2 by the removal of

lattice oxygen, a process which reduces and quickly deactivates the catalyst as surface oxygen is consumed. Conversely, NO is converted to N₂ on reduced SnO₂ surfaces through a process which reoxidizes the catalyst. Therefore, the formation and decomposition of oxygenates is dependent on the availability of lattice oxygen at the surface.

There is a close relationship between the SnO₂(110) surface characterization and the existing catalytic data on the selective isomerization of 1-butene to cis-2-butene (cis-/trans-2-butene = 19) over tin oxide powder [5]. Itoh, et al. [5] found that the activity and selectivity for cis-2-butene increased dramatically when the catalyst was activated by heating in vacuum to temperatures in the range of 400°C to 600°C (723 K to 823 K). Associated with this change was the appearance of electron-donating paramagnetic centers on the catalyst as seen by ESR. In the presence of 1-butene the ESR signal for this center decreased, indicating a direct interaction between 1-butene and the paramagnetic center. A direct correlation was found between the activity and selectivity of the catalyst and the concentration of paramagnetic centers.

Note that the temperature range and preparation conditions (i.e., heating in vacuum) associated with the catalyst activation is similar to that required to remove in-plane oxygen atoms and expose threefold-coordinated tin cations on the SnO₂(110) surface. The electronic properties of the in-plane oxygen vacancies have been described previously in terms of surface color centers [18] which act as electron donors. In the ground state the anion vacancies bind two electrons by their Coulombic wells, and are thus doubly ionizable. The first ionization potential of the defect is small (25 meV [25]); therefore, the majority of these centers are singly ionized and contain one unpaired electron as seen in the ESR signal. These similarities suggest that the isomerization reaction over powders occurs in the presence of sites similar to the in-plane oxygen vacancies observed on the SnO₂(110)-1x1 surface.

Itoh, et al. also observed that the catalyst is poisoned by a number of compounds including H₂O. The UPS results described above for water adsorption on the SnO₂(110) surface have shown that water preferentially adsorbs at in-plane oxygen vacancies on the SnO₂(110) surface. Hence, both the isomerization activity of SnO₂ powders and the poisoning capacity of water can be explained in terms of the properties of the defective SnO₂(110) surface.

REFERENCES

1. F.J. Berry, Adv. Catal. 30(1981)97.
2. D.J. Hucknall, Selective Oxidation of Hydrocarbons (Academic Press, New York, 1974).
3. S. Tan, Y. Moro-oka and A. Ozaki, J. Catal. 17(1970)125.
4. T. Sakamoto, M. Egashira and T. Seiyama, J. Catal. 16(1970)407.
5. M. Itoh, H. Hattori and K. Tanabe, J. Catal. 43(1976)192.
6. M.J. Fuller and M.E. Warwick, J. Catal. 29(1973)441.
7. G.C. Bond, L.R. Molloy and M.J. Fuller, J.C.S. Chem. Comm. (1975)796.
8. G.C. Bond, M.J. Fuller and L.R. Molloy, Proc. Int. Congr. Catal. 6th, 1(1977)356.
9. B. Hori, N. Takezawa and H. Kobayashi, J. Catal. 80(1983)437.
10. C.L. Lau and G.K. Wertheim, J. Vac. Sci. Technol. 15(1978)622.
11. T.W. Capehart and S.C. Chang, J. Vac. Sci. Technol. 18(1981)393.
12. W.E. Morgan and J.R. Van Wazer, J. Phys. Chem. 77(1973)964.
13. R.A. Powell, Appl. Surf. Sci., 2(1979)397.
14. D.F. Cox and G.B. Hoflund, Surf. Sci. 151(1985)202.
15. Z.M. Jarzebski and J.P. Marton, J. Electrochem. Soc. 123(1976)199,299,333.
16. V.E. Henrich, Rep. Prog. Phys. 48(1985)1481.
17. P.A. Cox, R.G. Egdell, C. Harding, W.R. Patterson and P.J. Tavener, Surf. Sci. 123(1982)179.
18. D.F. Cox, T.B. Fryberger and S. Semancik, Phys. Rev. B 38(1988)2072.
19. E. deFrésart, J. Darville and J.M. Gilles, Appl. Surf. Sci. 11/12(1982)637; Solid State Commun. 37(1980)13.
20. D.F. Cox, T.B. Fryberger and S. Semancik, Surf. Sci. 224(1989)121.
21. D.F. Cox, T.B. Fryberger, J.W. Erickson and S. Semancik, J. Vac. Sci. Technol. A 5(1987)1170.

22. D.F. Cox and T.B. Fryberger, Surf. Sci. Letters, 227(1990)L105.
23. M. Niwa, T. Minami, H. Kodama, T. Hattori and Y. Murakami, J. Catal. 53(1978)198.
24. F. Solymosi and J. Kiss, J. Catal. 41(1976)202.
25. J.W. Erickson and S. Semancik, Surf. Sci. 187(1987)L658.

OUTER ATOMIC LAYERS OF SnO_2

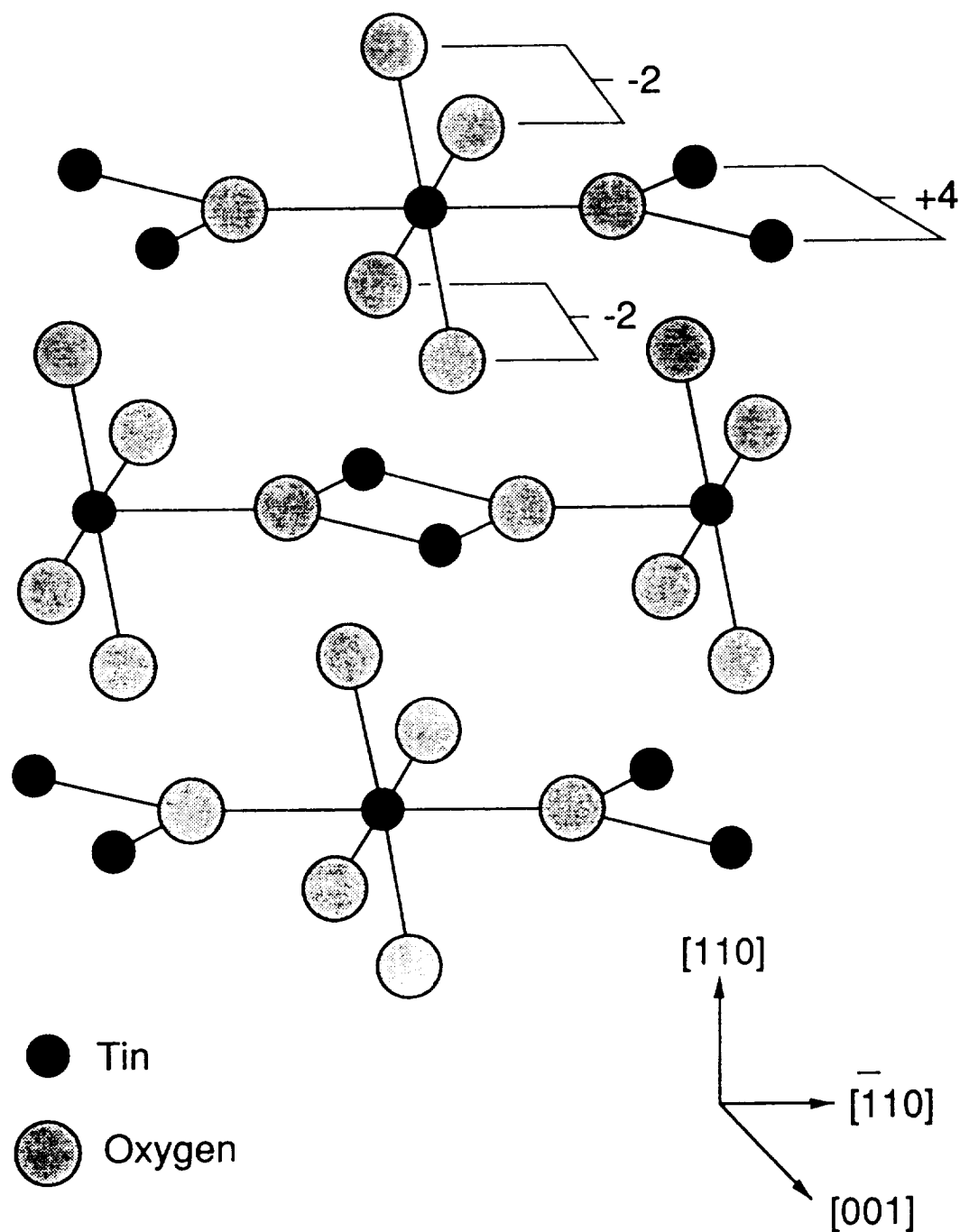


Figure 1. Illustration of the atomic arrangement at the ideal $\text{SnO}_2(110)-(1 \times 1)$ surface. The net charge per surface unit cell is shown for each of the three atomic planes composing a charge neutral unit perpendicular to the (110) direction. (Reproduced from Ref. 20, permission to reproduce granted.)

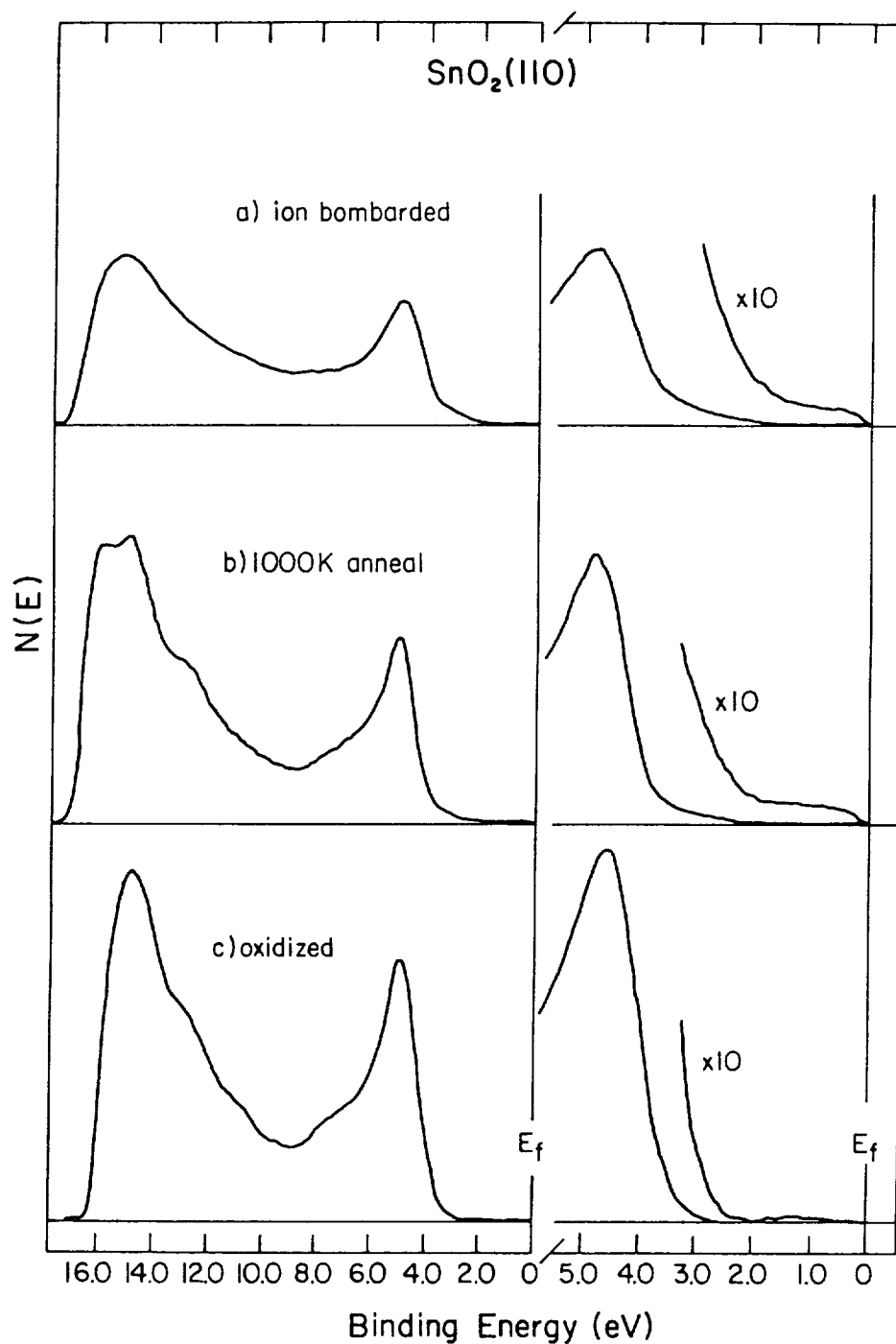


Figure 2. UPS spectra obtained following three different surface preparations: (a) 2-keV in bombardment, (b) ion bombarded and annealed in vacuum at 1000 K, and (c) oxidized in 1.0 Torr of O_2 at 700 K. The panels on the left are complete HeI spectra while the right-hand panels are enlarged views of the band-gap regions and the tops of the valence bands. All spectra are referenced to the Fermi level. (Reproduced from Ref. 18, permission to reproduce granted.)

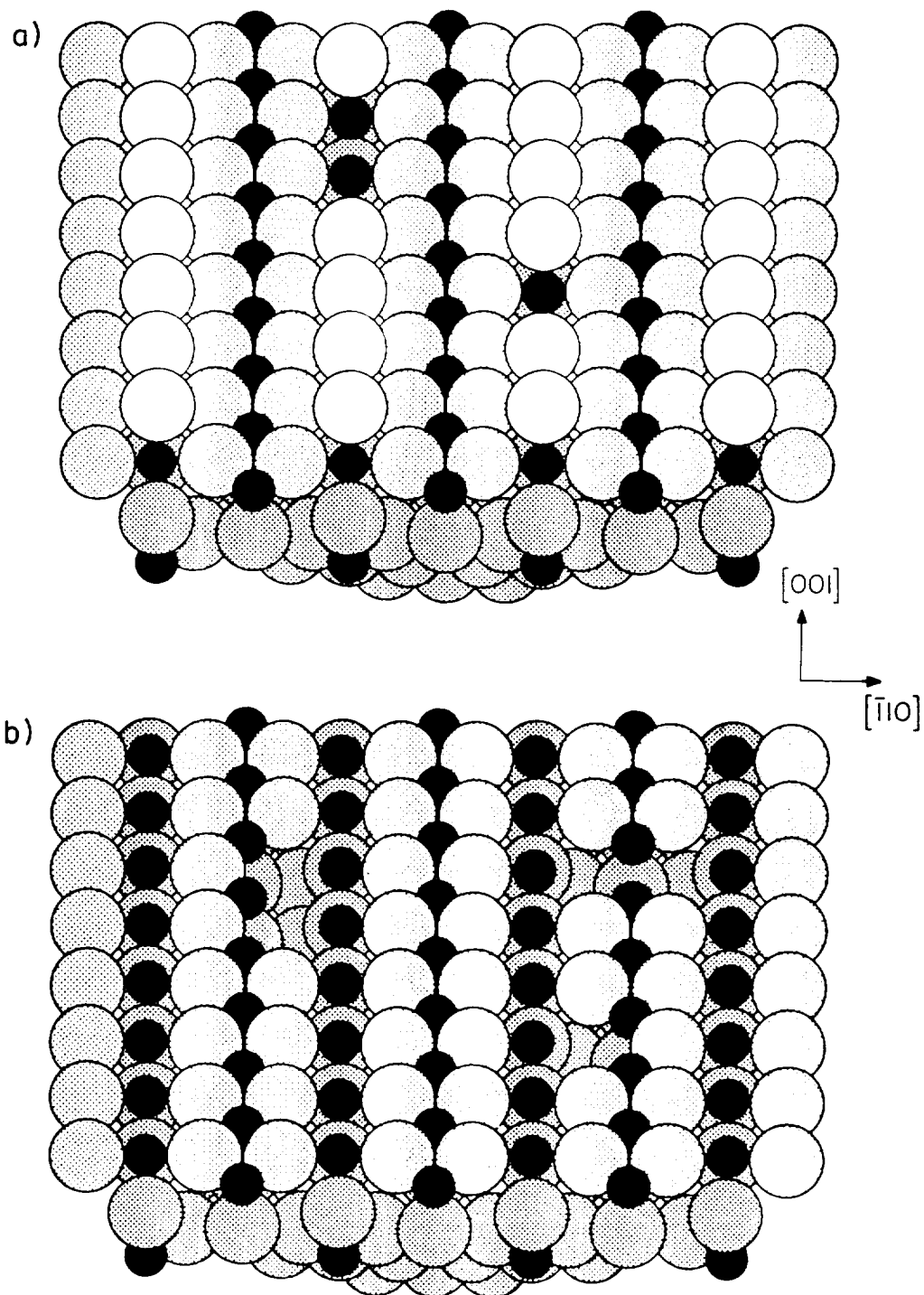


Figure 3. Ball model illustration of the surface viewed 50° off normal along the [001] azimuth. View (a) shows a nearly perfect (110) surface while (b) shows a bare surface following the removal of all top-layer bridging oxygen anions. A few in-plane oxygen vacancies are also shown in (b). (Reproduced from Ref. 18, permission to reproduce granted.)

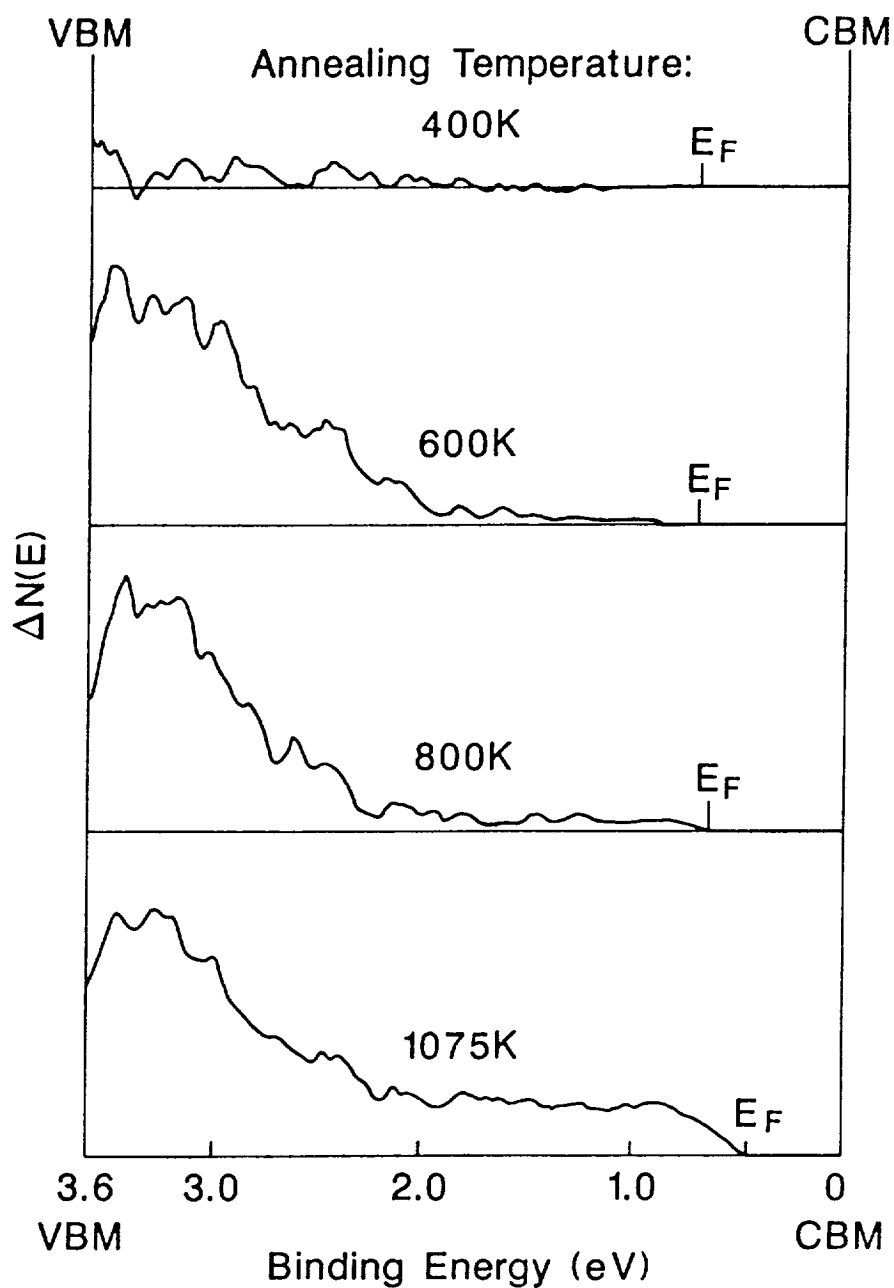


Figure 4. UPS difference curves showing the increase in band-gap (defect) electronic states caused by heating an oxidized surface in vacuum. The curves are referenced to the conduction band minimum (CBM). (Reproduced from Ref. 18, permission to reproduce granted.)

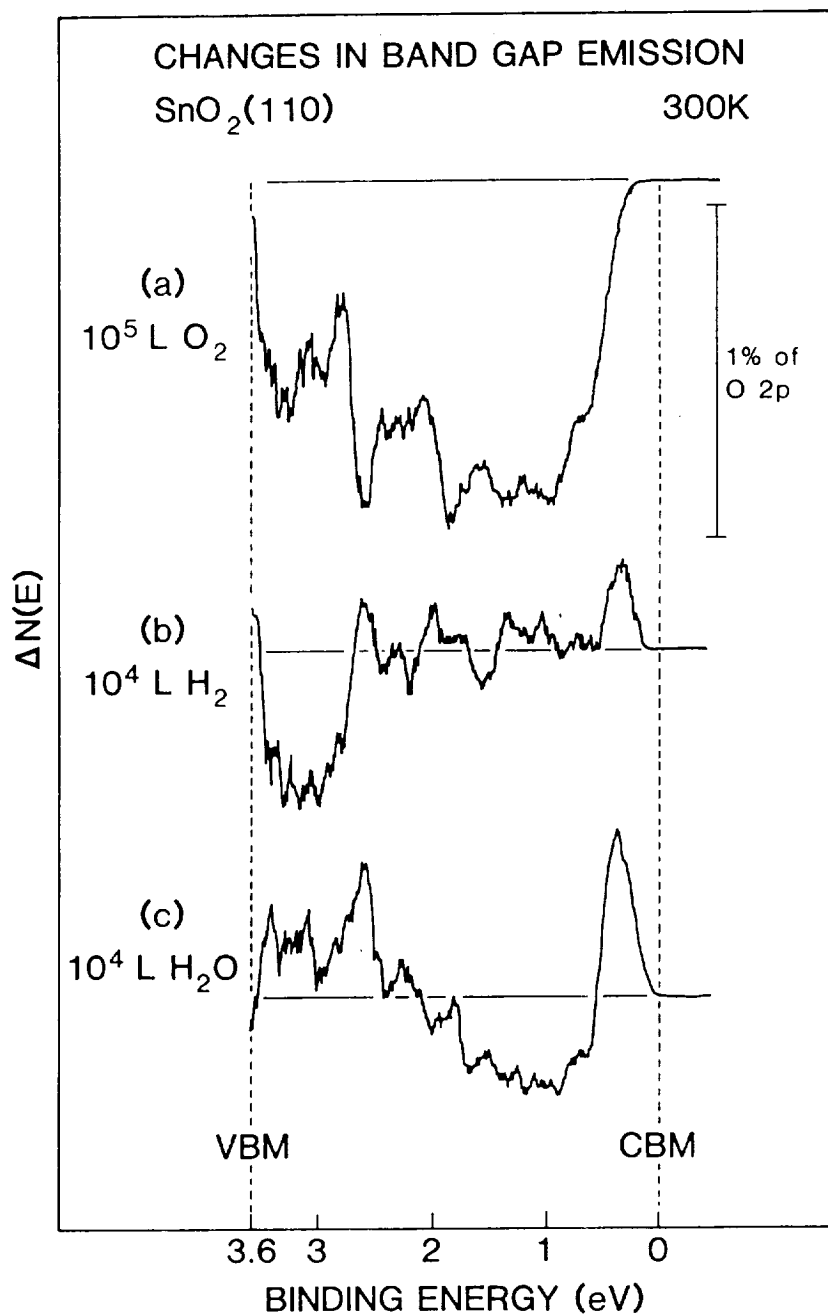


Figure 5. UPS difference curves indicating the changes in the band-gap density of states produced by adsorption of (a) 10^5 L O_2 , (b) 10^4 L H_2 , and (c) $10^4 \text{ L H}_2\text{O}$ on an ion sputtered surface. (Reproduced from Ref. 21, permission to reproduce granted.)

